كلية الهندسة بشبرا
FACULTY OF ENGINEERING AT SHOUBRA
ERJ
PRINT ISSN 3009-6049
ONLINE ISSN 3009-6022

ENGINEERING RESEARCH JOURNAL (ERJ)
Volume (54),Issue (1)
January 2025, pp:271-278
https://erjsh.journals.ekb.eg

Impact Of Utilizing Twin Jet Flow Methanol And Propane To Alter The Jet Forms In The Combustion Chamber

Mohamed Salah Yasein [1,*] , Ismail M.M. ElSemary [1] , Ahmed Attia Abd El Latief Attia Attia [1] , Mamdoh Eldosokey [1] , Maher Hegazy [1]

[1] Mechanical Engineering Department, Faculty of Engineering at Shoubra, Benha University, Cairo, Egypt.
**Corresponding author*

E-mail address: mohamed.salah01288018766@gmail.com, i.semary@feng.bu.edu.eg, ahmed.attia@feng.bu.edu.eg, masahkhab68@gmail.com, maherhigazy@yahoo.com

Abstract: This paper focuses on improving the combustion performance of a twin-jet intake without premixing. Using ANSYS software, we are examined how changes in fuel and air inlet shapes at different speeds impact combustion. Three main concepts were explored: turbulent flow, species transfer, and finite rate/eddy dissipation. The investigation centered on two intake jet designs—circular star and circular square. Findings showed that altering the inlet shape and velocity influences factors like equivalent ratios, temperature, heat release rate, and overall combustion efficiency.

Keywords: combustion, efficiency, heat release rate, equivalent ratios.

1. Introduction

Improving combustion efficiency calls for more investment in both research and real-world testing. Accurately predicting flame stability and emissions requires an advanced combustion model that factors in chemical reactions. To meet this needs for build them stronger, more reliable, and efficient numerical models. In high-speed propulsion systems, twin jets can be configured in various ways to reduce noise, control thrust direction, and improve performance.

Originally, circular twin jets were favored for production because they easily fit into gas turbine engines. However, as the demand grew for faster mixing, non-circular jets were developed, which helped increase mixing rates and improve system flexibility. Over the years, many studies have examined different aspects of combustion systems, particularly focusing on dual jet designs and how to maintain combustion stability.

Maele et al. [1] found that the realizable k- ϵ model performed slightly better, while adjustments to constants in the standard k-epsilon model improved results for certain flame types. Dally et al. [2] adjusted a constant within the dissipation transport equation of the standard $k-\epsilon$ model, leading to improved performance of the modified $k-\epsilon$ model when applied to bluff body flames, even surpassing that of the Reynolds Stress Model (RSM). Frassoldati et al. [3] further compared the RSM, the modified $k-\epsilon$ model, and the traditional $k-\epsilon$ model in similar contexts. Their analysis highlights the modifications' effectiveness in better capturing the flame dynamics around bluff bodies, offering an alternative to the more computationally intensive RSM.

Jing [4] research suggests that mixing whirling blade combustion with blade angles in a 1:1.25 ratio effectively reduces carbon monoxide and nitrogen oxide emissions in methanol combustion. Initially, circular twin ejectors were the most used because they were easy to manufacture, but rapid industrial demands pushed the need for non-circular jets. Also, Fiorina et al. [5] used a method based on premixed flames and probability density functions (PDF) to study high-speed flames with a wrinkled structure. They proposed a model that accounts for the interaction between flame fronts and micro-mixing. Other studies, like those by Muthuram, have provided insights into jet flow behavior and RANS modeling of turbulent combustion. For hydrogen-air and methane-air systems, researchers like Bray et al. [6] have explored simplified chemical reactions in high Damköhler number turbulent premixed flames, while Richardson examined the mixing times in 3-D simulations of methane-air flames, showing that steep flame fronts affect mixing rates. Richardson et al. [7] investigated the mixing time scale in three-dimensional Direct Numerical Simulations (DNS) using truncated CH_4-air chemistry, focusing on the confined reaction zone regime of turbulent Bunsen flames. Their study revealed that mixing rates are significantly influenced by the steep gradients formed by flame structures with high Damköhler numbers, which characterize the rapid chemical reactions compared to mixing processes. An in-depth analysis of various methods aimed at reducing the complexity of chemical kinetics, with a particular emphasis on combustion modeling. These works collectively highlight advancements in simplifying chemical reaction mechanisms without sacrificing accuracy in simulating turbulent combustion scenarios [8–12]. Tang et al. [13] developed a 3-D computational model to simulate H-air combustion in a micro-combustor for thermo-photovoltaic systems. Their work highlighted the role of wall radiation in achieving higher temperatures with improved designs. The thickened flame model is particularly useful for predicting pollutant formation in turbulent combustion. Gau et al. [14] further demonstrated how multistep reactions can be integrated with this model, showing incomplete combustion under both laminar and turbulent conditions. Natural gas, with its lower combustion efficiency, presents a challenge for high-pressure environments and can cause combustion instability compared to fuels like ASTM A-1 or propane, particularly in low-altitude ignition scenarios.

2. PROBLEM DEFINITION

This work investigates the combustion of twin non-premixed fuel jets (methanol and propane) injected through two inclined jets inside a cylindrical combustion chamber, with air supplied via a pipe. A centrifugal fan generates turbulent flow, and Ansys software models the combustion process. The investigate explores the effects of various factors like fuel velocity and jet geometry on combustion efficiency, Heat Release Rate (HRR), and equivalency ratios.

In this study, clean fuels were considered to enhance environmental sustainability. Given that twin jets exhibit distinct behaviors compared to single jets, several factors such as intake jet velocities and geometry(star and square shape as shown in figure 2) were taken into account, as these parameters significantly influence the mass flow rate and combustion characteristics. These factors, in turn, affect the shape, behavior, and overall performance of the combustion process. The modeling was developed using Ansys, supported by controlled experimental data. As shown in Table 1, the combustion chamber has a length of 110 mm, an outer diameter of 30 mm, and an inner diameter of 22 mm. The setup includes two input pipes: one for air and another for gases. A centrifugal fan with blades is used to monitor the gases optically.

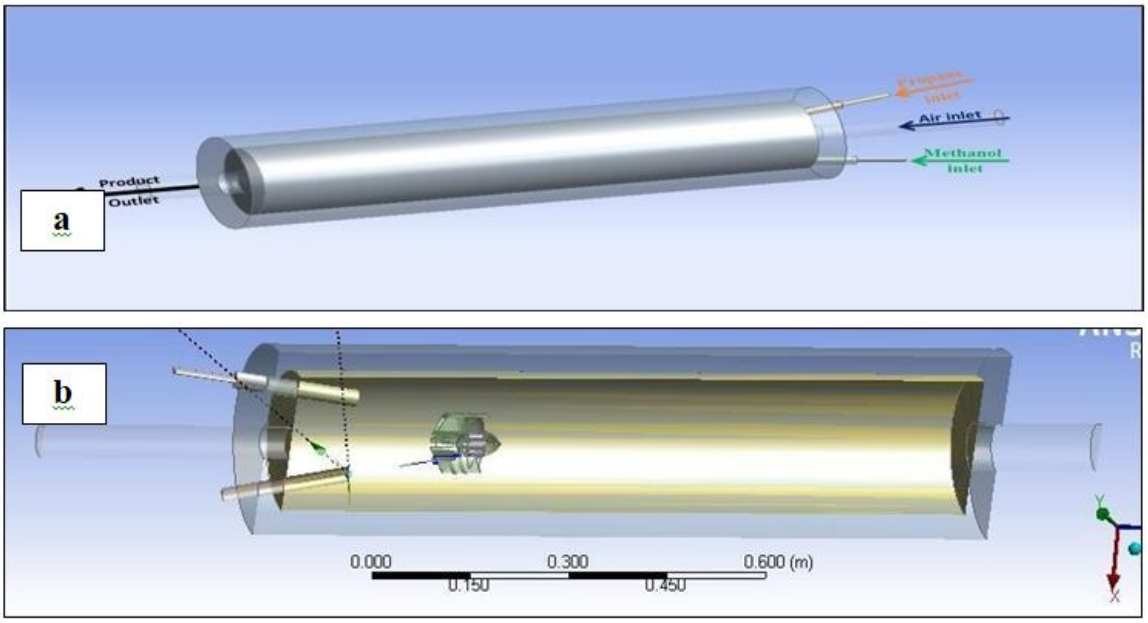

Figure 1: Twin non-premixed fuel jets CFD model.

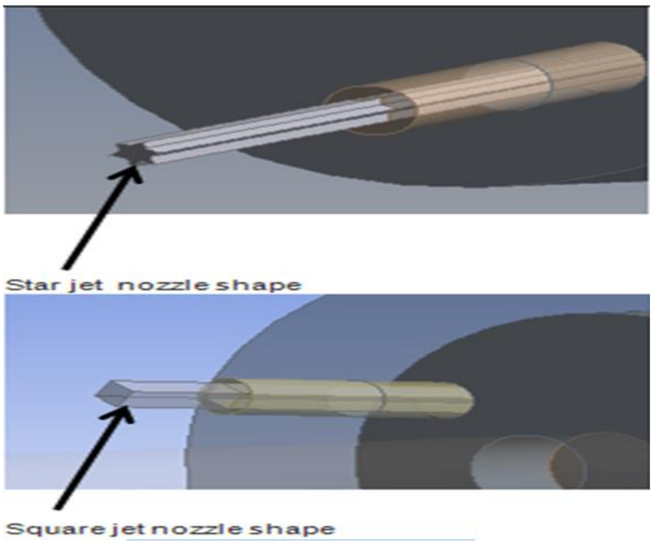

Figure 2 square and star jets shapes.

Table 1Combustion chamber specification.

Inner diameter of the combustion chamber	0.22m
ChamberD air pipe	0.05m
Djet propane	0.0258m
Djet methanol	0.02589m
Length of combustion chamber	1.1m
Outer diameter of the combustion chamber	0.30m

2.1 Mathematical Modeling

2.1.1 Turbulence Model

The standard two-equation, k-ε turbulence model with standard values was used for this study. The k-ε turbulence model consists of the turbulent kinetic energy and dissipation equations given below:

$$\frac{\partial k}{\partial t} + \nabla . (\rho \vec{u} k) = \nabla . \left\{ \left[\mu_{lam} + \frac{\rho\, \nu_t}{\sigma_k} \right] \nabla k \right\} + \rho \nu_t G - \rho \varepsilon \quad (1)$$

$$\frac{\partial \varepsilon}{\partial t} + \nabla .(\rho \vec{u}\varepsilon) = \nabla.\left\{\left[\mu_{lam} + \frac{\rho \nu_t}{\sigma_\varepsilon}\right]\nabla\varepsilon\right\} + C_{1\varepsilon}\rho\nu_t G\frac{\varepsilon^2}{k} - C_{2\varepsilon}\,\rho\frac{\varepsilon^2}{k} \quad (2)$$

where G represents the turbulent generation rate which is equal to

$$G = 2\left\{\left[\frac{\partial u}{\partial x}\right]^2 + \left[\frac{\partial v}{\partial y}\right]^2 + \left[\frac{\partial w}{\partial z}\right]^2\right\} + \left(\frac{\partial u}{\partial y} + \frac{\partial v}{\partial x}\right)^2 + \left(\frac{\partial u}{\partial z} + \frac{\partial w}{\partial x}\right)^2 + \left(\frac{\partial w}{\partial y} + \frac{\partial v}{\partial z}\right)^2 \quad (3)$$

$$\frac{\partial}{\partial t}(\rho Y_i) + \nabla.(\rho\vec{v}\nu\, Y_i) = -\nabla\vec{J}_i + Ri + Si \quad (4)$$

Where;

Ri = the net production rate of species i by chemical reaction and

Si = the rate of creation by addition from the dispersed phase and any other sources.

In the execution of this model the Kolmogorov-Prandtl expression for the kinematic turbulent viscosity, νt is used and it is given by:

$$\nu_t = C_\mu \frac{\varepsilon^2}{k} \quad (5)$$

In the equations above Cμ, σk, σϵ, C1μ, and C2μ are all taken to be constants and are given their usual standard values of: 0.09, 1.0, 1.3, 1.44 and 1.92 respectively.

The species were modeled using the model based on the work published by Westbrook and Dryer (1981). This simplified model consists of one chemical reaction and 5 species. The mixing and transport of chemical species can be modeled using Fluent-Ansys by solving the conservation equations that describes convection, diffusion and reaction for each element species. Simultaneous chemical reaction can be modeled here as a volumetric reaction.

The combustion process is modeled using the approach developed by Westbrook and Dryer (1981), which incorporates a simplified one-step chemical reaction mechanism involving five species. The model treats the chemical reactions as volumetric reactions and solves the conservation equations for each species, considering convection, diffusion, and reaction.

The mass fraction of each species, Yi can be obtained by solving the conservation equation for the i_{th} species that can be written as:

2.1.2 Mass diffusion in laminar flows

In laminar flows, the diffusion flux $\vec{J}i$ of species i in Eq. (1), which results from concentration and temperature gradients can be expressed as:

$$\vec{J}_i = -\rho D_{t,m}\nabla Y_i - D_{T,j}\frac{\nabla T}{T} \quad (6)$$

Where;

Di,m , DT,i are the mass and the thermal (Soret) diffusion coefficients respectively

2.1.3 Mass diffusion in turbulent flows

The mass diffusion in turbulent flow takes the form:

$$\vec{J}_i = -(\rho D_{t,m} + \frac{\mu_t}{SC_t})\nabla Y_i - D_{T,i}\frac{\nabla T}{T} \quad (7)$$

Where

Sct = the turbulent Schmidt number (Sct = μt /ρDt)

μt = the turbulent viscosity.

Dt = the turbulent diffusivity.

In many multicomponent mixing flows, the transport enthalpy due to diffusion of species is given by: $\nabla.\left[\sum_{i=1}^{n} h_i\vec{J}_i\right]$ which affect significantly when Lewis number is far from unity.

$$Lei = \frac{K}{\rho C_{pD_{i,m}}} \quad (8)$$

3.

3.1 Computational Domain and Grid

The computational domain includes a mesh for both the propeller gas and combustion zones. The 1 mm face mesh manages the propeller gas, while the 5 mm mesh represents the combustion chamber. The model generates additional bodies automatically during the simulation. In total, the grid consists of 44,225 nodes and 218,157 elements.

3.2 The Species Model

For species modeling, the Westbrook and Dryer (1981) mechanism was employed, which includes two species and two chemical interactions. To calculate the reaction rate, one of three available models in Fluent-Ansys was used: the laminar finite rate model, the eddy dissipation model, or the eddy dissipation concept. These models provide a comprehensive framework for predicting reaction rates, which appear as source terms in Equation (1). The boundary conditions applied in this research work are listed in Table 2, detailing the air/fuel, methanol/fuel, and propane/fuel inlet conditions. The equivalence ratio, which determines the species' mass fractions, was also calculated for the different fuel mixtures explored.

The outflow gauge pressure of the combustion gases is set to zero, while the backflow temperature is maintained at 923 K. The mass fractions of the outflow species are governed by the equivalence ratio, ensuring proper representation of the combustion products. For the wall boundary conditions, no-slip adiabatic conditions are applied, which means that the velocity of the gas at the wall surface is zero, and no heat transfer occurs across the wall boundaries

Table 2 Inlet conditions of the combustion chamber

Inlet	Inlet velocity ofthe air pipe (m/s)	Turbulence intensity	Turbulencelength scale (m)	Inlet temperature (K)
Air	2.5,5,6 and 12	3.6 %	0.003	298
Methanol	1.2,1.5,2 and 2.22	3.6 %	0.003	298
Propane	1.2,1.5,2 and 2.22	3.6 %	0.003	298

4. SOLUTION METHOD

4.1 Stability and Convergence

Due to the strong coupling between the mass, momentum, and species transport equations in reacting flow, finding a convergent solution is challenging. This difficulty is compounded by the intense heat release from chemical reactions, which leads to significant shifts in density and rapid flow acceleration. The presence of a "stiff" system, where reaction kinetics outpace convection and diffusion, adds further complexity to solving species transport equations. To address these issues, a two-step solution technique is implemented. Initially, the reaction is blocked, and a "cold" or non-reacting flow solution is obtained. Once the flow pattern stabilizes and starts resembling the basic flow, the reaction is activated. This staged approach helps avoid convergence problems caused by the coupling of chemical reactions with fluid flow.

In laminar flow scenarios, a coupled solution is recommended, while for turbulent flows, the eddy dissipation concept (EDC) is preferred to model the interaction between turbulence and chemical reactions. The EDC approach allows for better simulation of the reaction rate in turbulent flows. For ignition, the process is similar to spontaneous combustion, where fuel and air must reach a temperature above the activation energy threshold. In the simulation, a high-temperature region (1000 K) is initialized in the combustion domain to act as a "spark" for ignition. The results show that this initial condition does not affect the final steady-state solution. The spatial discretization uses the gradient least square cell-based method for gradients and the second-order upwind scheme for density, momentum, and modified turbulent viscosities. Additionally, relaxation factors are applied to improve stability: 0.8 for species, energy, and density, and 0.6 for momentum, turbulent kinetic energy, turbulent dissipation rate, and turbulent viscosity. This combination of techniques ensures a stable and convergent solution in the reactive flow simulation

5. Model Validation

To evaluate the reliability of the current model, its predictions were compared with those from previous studies by Jing et al. [11], Muthuram [12], and Anetor et al. [13]. The numerical analysis of the effect of fuel equivalency ratio and swirl angle on methanol combustion characteristics in a swirl burner shows a fair degree of consistency, as seen in Figure 3. This agreement suggests that any small variations in the results could be attributed to differences in the geometry dimensions of the models.

Using the same boundary conditions and combustion chamber dimensions as Jing et al. [11], our model produced similar results, supporting the validity of the approach. Motivated by the findings of Jing et al. [11], we further utilized Muthuram [12] to determine the swirl blade angle at 60º+60º, which was applied after the jets in the combustion chamber. This configuration creates turbulence in the gas mixture from the inlet jets. The comparison between these studies, particularly the blade angle configuration BA2 (60º+60º), as shown in Figure 4, reveals that while minor differences arise due to chamber dimensions, the overall trends remain consistent. This reinforces the reliability of the current model in simulating combustion behavior in swirl burners.

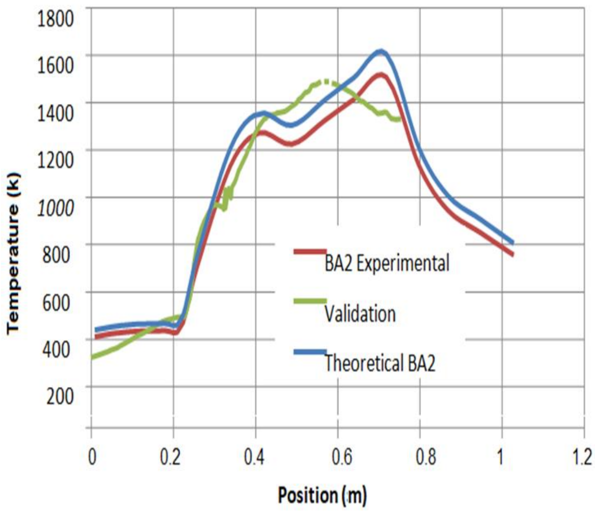

Figure3: Comparison between the theoretical and experiment of Jing et al. [11] work with my validation.

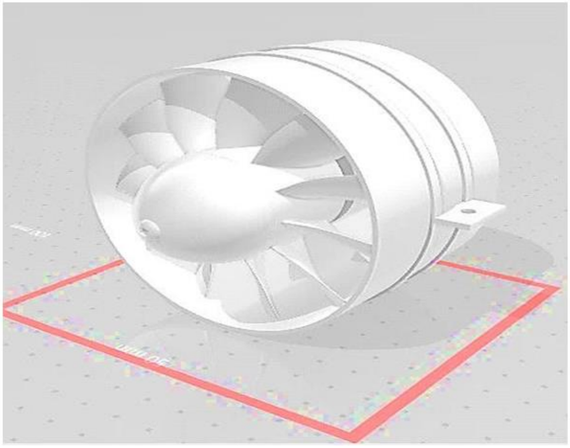

Figure 4. Blade angel 60º+60º as in Jing et al. [11].

As illustrated in Figure 5, the temperature distribution obtained in this study matches the validated results when applying the search parameters from Jing et al. [11]. The flame shape predicted by the model in Figure 5aligns closely with the validation by Jing et al. [11], showing consistency in both the elevation - and plan views. This validation confirms that our model accurately replicates the flame structure and behavior under similar conditions, further supporting its reliability in simulating combustion characteristics.

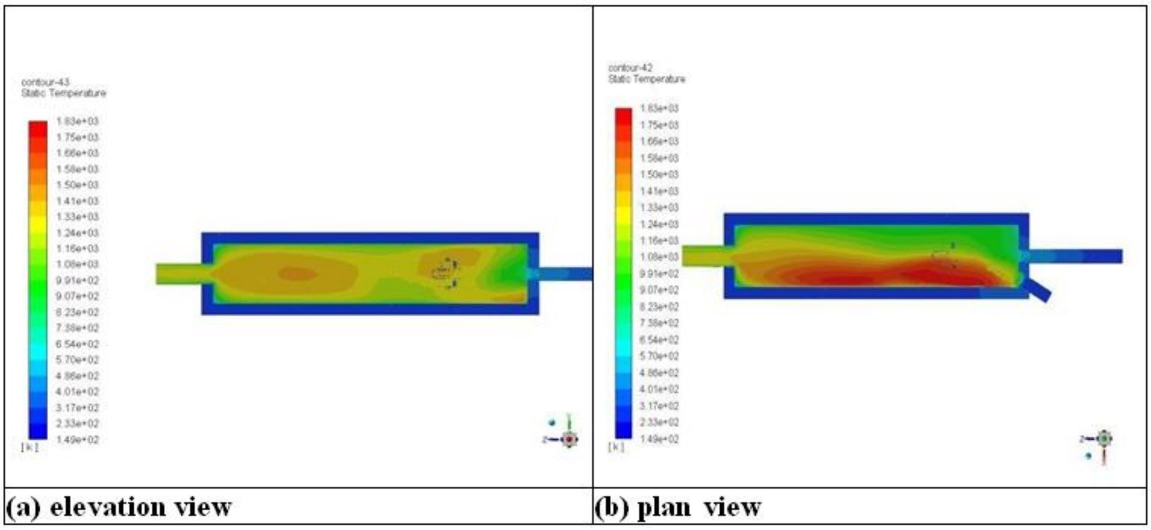

Figure 5 Flame Shape according to the computational model.

6. Combustion Performance

6.1 Parameters Combustion Efficiency

The combustion efficiency is calculated as follows:

The combustion process produced heat Q_{fuel}, Q_{heat}, and Q_{air}, where Q_{heat} denotes the output heat and Q_{fuel} and Q_{air} are the inputs.

$$Q_h = mg\ Cpg\ (T_{go}-T_{airi}) \quad (9)$$

$$Q_{air} = m_{air} cp_{air}\ (T_{out} - T_{gi}) \quad (10)$$

$$Q_{input} = (m_f \times Lcv) + Q_{air} \quad (11)$$

So, the efficiency of the combustion process can be expressed as:

$$\eta = \frac{Q_h}{Q_{input}} \quad (12)$$

The mass fraction of each species YiY_i is determined by solving the species transport equation:

$$\frac{\delta}{\delta t}(\rho Y_i) + \nabla.(\rho V Y_i) = -\nabla.j_i + R_i + S_i \quad (13)$$

where Ri is the net production rate of species ii due to chemical reactions, and Si S_i accounts for the rate of creation from the dispersed phase and other sources.

Additionally, for the modeling of species transport, mass diffusion is considered in both laminar and turbulent flows. In turbulent flows, the species diffusion flux is expressed as:

$$J_i = -\left(\rho D_{t,m} + \frac{\mu_t}{S_{Ct}}\right)\nabla Y_i - D_{T,i}\frac{\nabla T}{T} \quad (14)$$

This includes the contribution of turbulent viscosity (μt\mu_t) and turbulent diffusivity (DtD_t), with the Schmidt number SCtS_{C_t} characterizing the effect of turbulence on species diffusion.

We hope this clarification enhances the description of the combustion model and addresses your concerns. If further clarification is needed, we are happy to provide additional details.

6.2 Heat Release Rate

The heat release rate HRR is calculated from:

$$HHR = \frac{Q_{release}}{A_S} \quad (15)$$

, where, As is the unit surface area of the combustion chamber and

$$Q_{release} = Q_{fuel} + \frac{Q_{air}}{2} \quad (16)$$

7. RESULTS AND DISCUSSIONS

The results were analyzed in two main sections firstly the impact of the Star Configuration examined how the star configuration affects temperature, efficiency, heat release rate (HRR), and equivalency ratios. It was found that variations in the star configuration influence these parameters significantly, demonstrating how different configurations can affect combustion efficiency and performance metrics. Secondly, the influence of

the Square Form of the Input Pipe focused on the effect of the square shape of the input pipe on air and fuel velocity fluctuations. This analysis was conducted across various temperatures, efficiencies, and equivalency ratios. The findings indicate that the shape of the input pipe can significantly impact the velocity fluctuations of air and fuel, which in turn affects the combustion temperature, efficiency, and heat release rate (HRR). Overall, both types of configurations influence combustion characteristics such as efficiency, HRR, and equivalency ratios, demonstrating the complex interplay between geometry, flow dynamics, and combustion performance.

7.1 Square shape

7.1.1 Effects of change velocity on efficiency, HRR, and equivalent ratios

In the study of the relationship between velocity and combustion within the lean-to-chemically correct gas mixture range, as depicted in Figure 6, the graph illustrates how the ratio of air velocity (V_{air}) to fuel velocity (V_{fuel})

impacts various combustion parameters. By inputting the velocities of the two fuel pipes and the air pipe into an Excel sheet, the ratio is analyzed against efficiency, HRR, and other factors. The analysis reveals a 19% gain in efficiency at V_{air}=12 m/s and V_{fuel}=1.5 m/s, followed by a 20% decline as the ratio changes, with a peak 30% increase when V_{air} =5 m/s and V_{fuel}=1.5 m/s. Additionally, Figure 8 shows that equivalency ratios increase linearly with the percent velocity of reaction products, exhibiting fluctuations until the reaction zone is reached. These results highlight the importance of optimizing the air-to-fuel velocity ratio to maximize combustion efficiency and understand its dynamic effects on the reaction process. It is clear in figure 6 that there is a drops in the efficiency in velocity ratio, this drops occurred because the centrifugal fan acted as a barrier after the gas exited the jets.

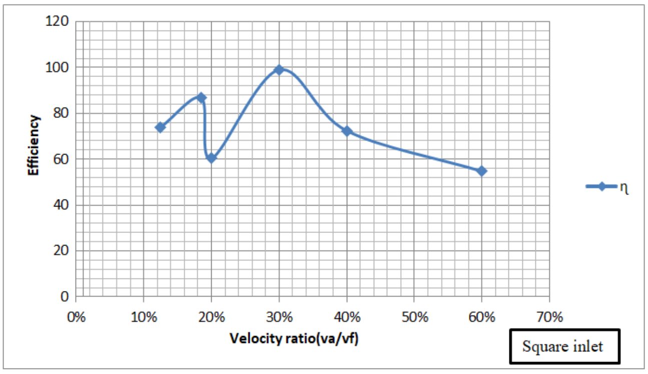

Figure 6: Relation between efficiency as (Y-axis) and percent of (velocity of air/velocity of fuel) as (X-axis).

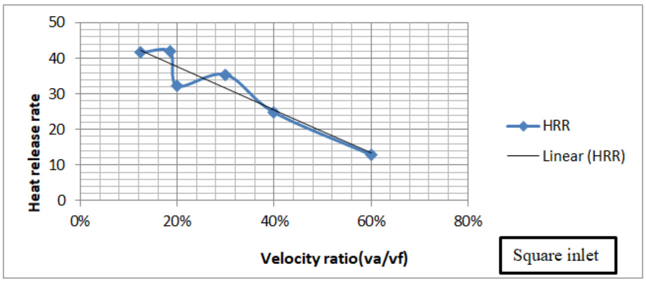

Figure 7: Relation between Heat release rate as (Y-axis) and percent of (velocity of air/velocity of fuel) as (X-axis).

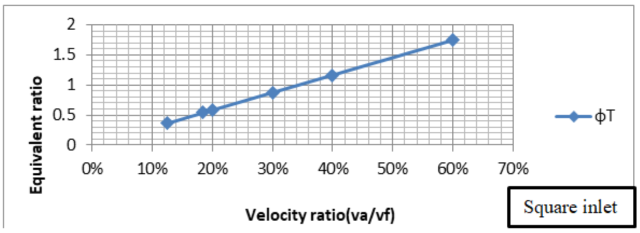

Figure 8: Relation between Equivalent ratio as (Y-axis) and percent of (velocity of air/velocity of fuel) as (X-axis).

7.1.2 Effects of methanol, propane, and air temperature at the in the square inlet

Figure 9 shows the effects of methanol, propane, and air temperature on combustion at the entry, depicting the temperature distribution along the centerline of the combustion chamber. The figure reveals that as the inlet temperature decreases, the combustion process initiates closer to the mixture inlet, leading to an increase in the product temperature. The temperature curve rises until it reaches 1100 K, with the variance in velocity corresponding to the temperature. Figure 10 further demonstrates the flame shape in the combustion chamber at V_{air} =12 m/s and V_{fuel}=2.22 m/s.

Additionally, the velocity significantly influences the combustion process, affecting overall combustion dynamics and flame characteristics.

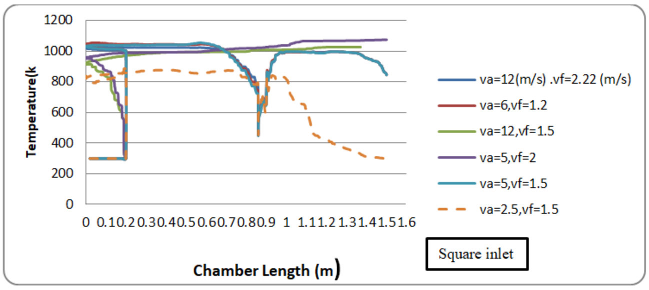

Figure 9: Effect of a velocity change on temperature and combustion chamber length in sqare inlet.

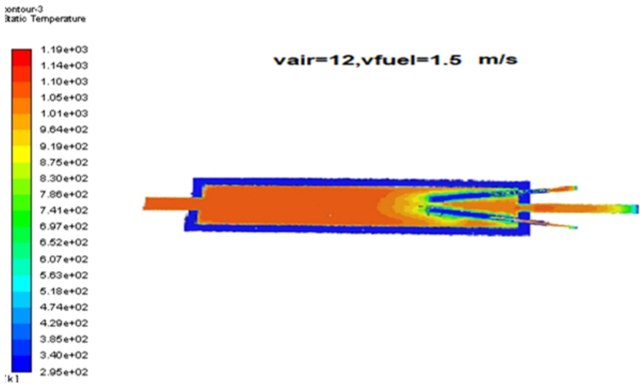

Figure10: Shape of fire along the center line of the combustion chamber.

7.2 Star form

Altering the shape of the inlet jet pipes, such as varying one of the three inlet pipes to a star or square configuration, affects the results and values as demonstrated. This modification changes the flow characteristics and combustion dynamics, leading to different outcomes in the temperature distribution, flame shape, and overall combustion performance.

7.2.1 Effects of change velocity on efficiency, HRR, and equivalent ratios

Variations in the form and velocity of the input pipes, as shown in Figure 11, significantly influence efficiency changes. The efficiency ratings deviate notably from the square form, with efficiency initially increasing by 13% before reaching a peak. After this point, efficiency saw a sharp decrease as velocity ratios increased. Specifically, it dropped by 20% at a velocity ratio of (V_{air} = 12, V_{fuel} = 1.5) and further reduced to 39% at a 60% velocity rate, or (V_{air} = 2.5, V_{fuel} = 1.5).

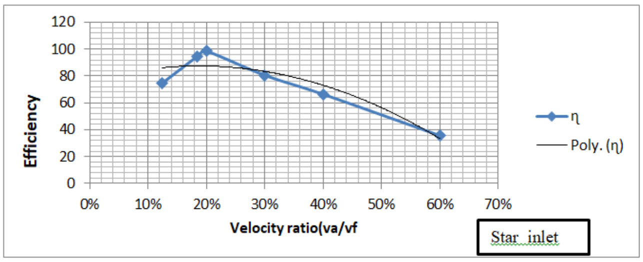

Figure 11: Relation between efficiency as (Y-axis) and percent of (velocity of air/velocity of fuel) as (X-axis).

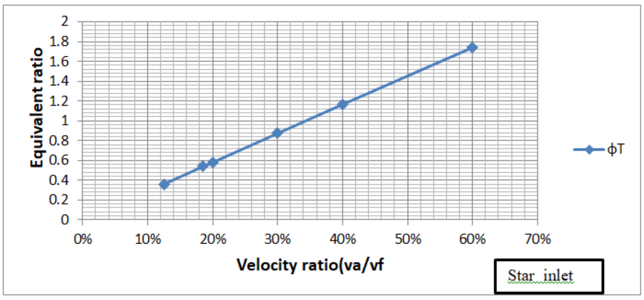

Figure 12: Relation between equivalent ratio as Y-axis and percent of velocity X-axis.

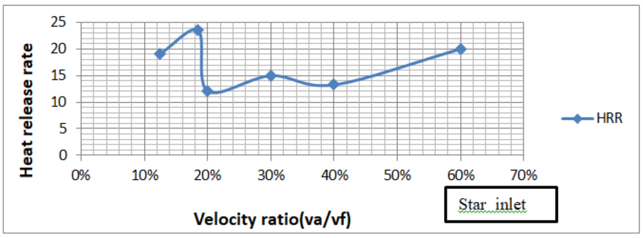

Figure 13: Relation between heat release rate and percent of velocity.

Likewise, Figure 12 shows a rise in efficiency under certain conditions. The relationship between the heat release rate (HRR) and the velocity ratio is illustrated in Figure 13. Initially, the HRR increases at a velocity ratio of 13%, rises further to 18%, and then fluctuates after 20%, eventually stabilizing at lower values. The HRR values for the square and star configurations differ significantly, but both follow a similar curved pattern. As depicted in Figure 13, with the heat release rate on the y-axis and velocity ratio on the x-axis, the HRR rises and then falls with varying velocity ratios. Notably, the rate of heat emission sees a distinct increase when the velocity ratio reaches 13%.

7.2.2 Effects on the intake of methanol, propane, and air temperature

Figure 14 illustrates the relationship between the length of the combustion chamber (x-axis) and the temperature exiting the chamber (y-axis), with distinct color curves representing the percentage of velocities (V_{air}/V_{fuel}). It highlights how variations in the velocities and shapes of the methanol and propane inlet pipes influence the combustion process by modifying the temperature distribution along the chamber's centerline. At V_{air} = 2.5 m/s and V_{fuel} = 1.5 m/s, the temperature declines, which differs from other velocity values, showing a unique process. Notably, the temperature drops lower than the square configuration. Figure 15 further demonstrates the flame's shape inside the combustion chamber post-combustion.

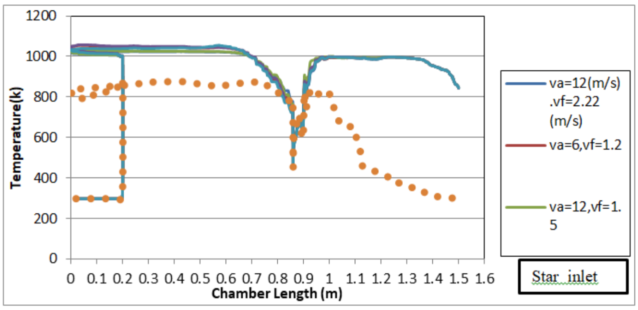

Figure 14 Effect of a velocity change on temperature and combustion chamber length (m).

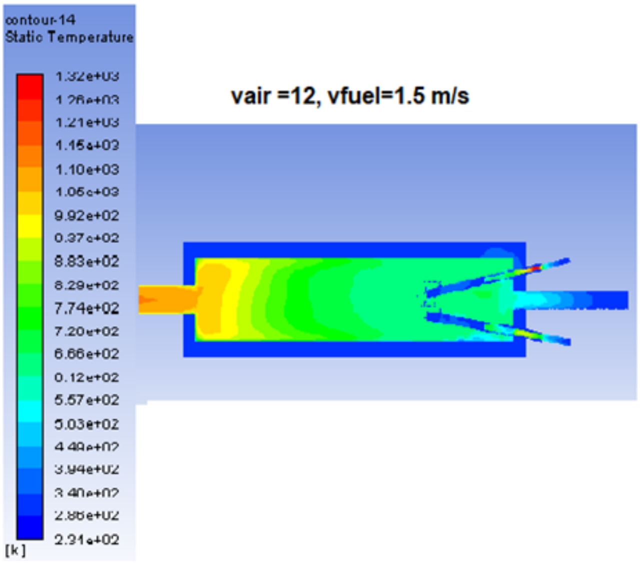

Figure 15: The shape of fire along the center line of the combustion chamber.

CONCLUSIONS

The experimental results indicate distinct differences between the impacts of using a circular-star intake jet and a circular-square inlet jet on temperature, heat release rate (HRR), efficiency, and equivalency ratio. From the study, it can be concluded that:

- The circular-star jet and circular-square jet produce different temperature distributions in the combustion chamber. The circular star jet shows a more favorable temperature profile across various velocities, indicating it may be more effective in certain conditions while the circular star jet shows a slightly different HRR pattern compared to the circular-square jet.
- Both jets show a rising trend in HRR, followed by fluctuations at higher velocity ratios, with the circular star jet exhibiting higher peak values at specific velocity ratios.
- The circular-square jet experiences a significant reduction in efficiency at higher velocities, whereas the circular-star jet shows more stable performance.

- Velocity ratios greatly influence combustion characteristics where the velocity ratio of 2.5/1.5 for the circular-star jet achieves the lowest recommended velocity. Other velocity values show better performance for both jet shapes, but this specific ratio is a critical point for the design and operational limitations.
- The flame formed by the **circular star jet** appears more stable and efficient under a variety of conditions compared to the circular square jet, which exhibits a steeper temperature decline in some instances.
- Based on the results, both the circular-star and circular-square jet shapes are suitable for most velocities tested. However, for the velocity ratio of 2.5/1.5, the circular-star jet is the recommended shape due to its lower temperature at this ratio, which suggests better combustion control and efficiency at low velocities.

These points highlight the detailed influence of intake jet shape and velocity on the combustion process, helping guide the selection of optimal jet configurations for efficient combustion.

AVAILABILITY OF DATA AND MATERIALS

The datasets used and/or analyzed during the current study are available from the corresponding author upon reasonable request.

REFERENCES

[1] In Hydrogen Energy 43.33 (2018), 16364–16372 are mentioned.2017; Acta astronautica 137: 403–414.6. (2015), pp. 104–115; Case Studies in Thermal Engineering 6;

[2] published 10.1016/j.matpr.2017.06.323; 10.18186/thermal.840007); 10.1166/jmihi.2015.1500; 10.1016/j.matpr.2017.06.323; 10.18186/thermal.840007

[3] B.B. Masri, Dally ,A.R., and Fletcher, D.F. 1998. chaotic bluff-body jet flow and mixing fields with flames. p. 193, Combustion Theory and Modelling, 2 (2).

[4] Maele, Merci, Dick, and B. (2003). A comparative analysis of k-epsilon turbulence models in swirlingflows that are inert and reactive. On page 3744 of the 33rd AIAA Fluid Dynamics Conference and Exhibit.

[5] T., Cuoci, Faravelli A., Sharma, P., Fassoldati, A., and Ranzi, E. (2010). Methane/hydrogen jet flame modeling in diluted coflow using kinetic and fluid dynamics methods. 30(4) of Applied Thermal Engineering,pp. 376–383.

[6] B. Carpentier, Fiorina, S. Gicquel, O., Vervisch, L., and Darabiha, N. (2005). PDF and tabular complete chemistry for premixed turbulent combustion modelling. The Combustion Institute Proceedings, 30(1), pp. 867–874.

[7] K. Champion , M. and Libby In 2010, Bray, K., Champion, P.A. Reduced rate mechanisms in a systematic manner and assumed PDF models for mixed turbulent combustion. Flame and Combustion, 157(3), 455–464.

[8] R.W. Chen ,Chen, J.H. Sankaran, R., and Richardson, E.S. (2010). The impact of reaction-diffusion on species mixing rates in turbulent premixed methane-air combustion is analyzed numerically. Pages. 506–515 inCombustion and Flame, 157(3).

[9] In Verbrennung und Feuerung, 24. Deutscher Flammentag, Bochum, September 16, 17, 2009, pp. 579–582).VDI Publishing.

[10] Hou, Z., Xu, Y., Yang, W., Pan, J., and Tang, A. (2015). The combustion of premixed hydrogen and air ina tiny planar combustor with parallel separating plates is studied numerically. Journal of Hydrogen Energy International, 40(5), pages 2396–2403.

[11] S. Wang, J., Wei, X., Yu, S., Zhang As of 2018, Guo, , Yu, S., Zhang, M., and Huang, Z. Premixed combustion numerical simulation with a multi-step reaction mechanism and a modified dynamic thickening flame model.233 Fuel, pp. 346–353.

[12] User's Guide for ANSYS Fluent. ANSYS, Inc., Release 15.0, November 2013.

[13] Du, Y., Zhu, Q., Jing, L., Zhao, J., Wang, H., and Zayed, M.E., 2022. The impact of fuel equivalency ratio and swirl angle on the combustion parameters of methanol in a swirl burner is analyzed numerically. 320–330 in Process Safety and Environmental Protection, 158.

[14] A. Muthuram. (2019). investigation of the effects of nozzle geometry on the properties of twin jet flow,Chennal, ANNA University, Mechanical Engineering Faculty 600 025

[15] E. Anetor, L. Osakue and C.Odetunde, , 2012. Reduced mechanism approach of modeling premixed propane-air mixture using ANSYS Fluent. Engineering Journal, 16(1),pp.